Photosensitive Triethoxysilane Derivatives for Alignment of Liquid Crystals

J. Naciri, J. Y. Fang,*,† M. Moore,*,† D. Shenoy, C. S. Dulcey, and R. Shashidhar

Center for Bio/Molecular Science and Engineering, Code 6950, Naval Research Laboratory, Washington D.C., 20375

Received July 25, 2000. Revised Manuscript Received September 11, 2000

Synthesis of a new class of triethoxysilane materials for photoinduced orientation of liquid crystals is reported. A feature of these silanes is the incorporation of a photosensitive chromophore in the chemical structure. This leads to the formation of a complete monolayer with smooth surface morphology. The effect of varying the chemical structure on the kinetics of monolayer formation as well as on the alignment of liquid crystals is discussed. Short hydrocarbon chains at the far end of the silane molecule lead to a uniform planar alignment while longer chains induce a perpendicular alignment of liquid crystal molecules.

Introduction

Liquid crystal displays (LCDs) are currently used for a variety of flat panel display applications. A crucial requirement of the LCDs is that liquid crystal (LC) molecules should be preferentially oriented along a uniform direction. This is achieved by a treatment of the substrates (directly in contact with LC molecules) with an alignment layer that dictates the orientation of the LC molecules. Current LCDs use rubbed polyimide as the alignment layer. However, a number of potential problems arise from this technique and continuous effort has been devoted to developing alternative alignment methods. In recent years, photoalignment techniques of LC molecules on substrates have been attracting great interest from a practical viewpoint because this is a nonrubbing process.[1−6] For the most part, these rubbing-free techniques involve exposure of spin-cast photopolymers to polarized UV light to control the LC alignment. In particular, photoalignment of LCs using poly(vinylcinnamate) systems has been extensively studied.[2−8] (See ref 6 for an excellent review on the subject).

We reported recently a new alignment layer based on self-assembled monolayers of silane-based cinnamate moieties.[9−11] This process, shown schematically as Path I in Scheme 1, consists of three steps: (i) chemisorption of a silane monolayer (shown as A), (ii) attachment of the photoreactive cinnamate groups via an amide linkage (shown as B), and (iii) irradiation of the chromophore with linearly polarized light. Irradiation by polarized UV radiation leads to the formation of dimers wherein adjacent molecules are bound together by the cyclobutyl group. This process of photoinduced dimerization leads to an aniosotropic surface that in turn aligns the LC molecules along a direction perpendicular to the direction of the polarization of the UV radiation. It has also been shown that this photodimerized monolayer (PDML) leads to an extremely uniform orientation of the LC molecules.[9−11] Also, LCDs made using the PDML layer are shown to have electrooptic properties that are similar to those that are fabricated using the rubbed polyimide as the alignment layer.[11] However, there are a few important issues that need to be addressed before the PDML is technologically feasible for LCDs. The first issue concerns the number of steps involved in the fabrication of the PDML. As seen in Scheme 1, this involves three steps, the formation of a monolayer, chemical attachment of a photosensitive group, and photoirradiation. From the manufacturing point of view, it is preferable to reduce the first two steps (involving formation of photoalignment layer) into a single step. The second issue concerns the reproducibility of monolayer fabrication itself. There is a fundamental problem associated with the self-assembly of aminopropyltriethoxysilane (APS) (shown as step A, path I) on surfaces. The structure of the APS film is complex, in that there are many possible conformations and orientations of the molecule with respect to the surface that can be realized.[12−19] The surface coverage

* To whom correspondence should be addressed.
† Also at GeoCenters Inc., 1801 Rockville Pike, Rockville, MD 20852.

(1) Gibbons, W. M.; Shannon, P. J.; Sun, S. T.; Swelin, B. J. *Nature* **1991**, *351*, 49.
(2) Schadt, M.; Schmitt, K.; Kozinkov, V.; Chigrinov, V. *Jpn. J. Appl. Phys.* **1992**, *31*, 2155.
(3) Chen, J.; Boss, P. J.; Bryant, D. R.; Johnson, D. L.; Jamal, S. H.; Kelly, J. R. *Appl. Phys. Lett.* **1995**, *67*, 1990
(4) Yamamoto, K.; Hasegawa, M.; Hatoh, H. *Proc. SID 96 Digest* **1996**, 642.
(5) Schadt, M.; Seiberle, H.; Schuster, A. *Nature* **1996**, *381*, 212.
(6) Ichimura, K. *Chem. Rev.* **2000**, *100*, 1847.
(7) (a) Seo, D. S.; Kobayashi, S. *Mol. Cryst. Liq. Cryst.* **1997**, *301*, 57. (b) Seo, D. S.; Hwang, L. Y.; Kobayashi, S. *Liq. Cryst.* **1997**, *23*, 923. (c) Seo, D. S.; Oh-Ide, T.; Kobayashi, S. *Mol. Cryst. Liq. Cryst.* **1992**, *214*, 97.
(8) (a) Imura, Y.; Kusano, J.; Kobayashi, S.; Aoyagi, Y.; Sugano, T. *Jpn. J. Appl. Phys.* **1993**, *32*, L93. (b) Imura, Y.; Saitoh, T.; Kobayashi, S.; Hashimoto, T. *J. Photopolym. Sci. Technol.* **1995**, *8*, 257.
(9) Shashidhar, R.; Grüneberg, K.; Shenoy, D.; Karkarla, U.; Naciri, J. *SID 97 Digest Techn. Pap.* **1997**, *28*, 315.
(10) Shenoy, D.; Grüneberg, K.; Naciri, J.; Chen, M. S.; Shashidhar, R. *SID'98 Digest Techn. Pap.* **1998**, *29*, 731.
(11) Shenoy, D.; Grüneberg, K.; Naciri, J.; Shashidhar, R. *Jpn. J. Appl. Phys. A* **1998**, *37*, *11*, L1326.
(12) Caravajal, G. S.; Leyden, D. E.; Quinting, G. R.; Maciel, G. E. *Anal. Chem.* **1988**, *60*, 1776, and references therein.

10.1021/cm000606m CCC: $19.00
Published on Web 11/02/2000

Scheme 1

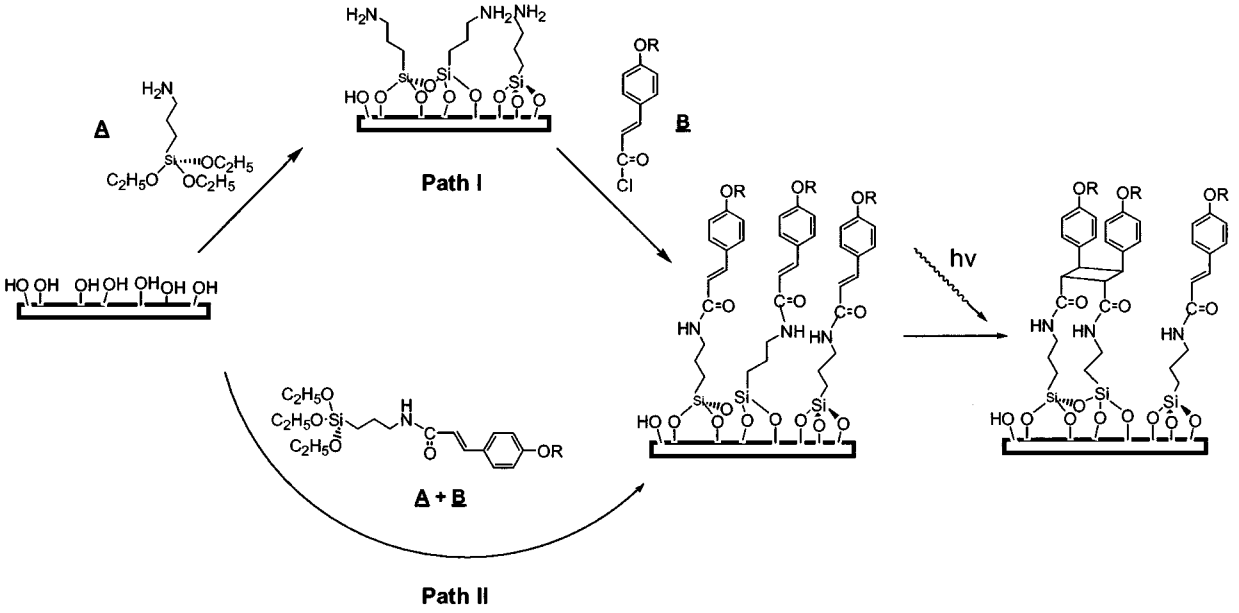

and structure depend sensitively on experimental parameters such as the reaction time, temperature, choice of solvent, and silane concentration.[19,20] If the film is deposited from a dry organic solvent such as toluene, there is an initial rapid adsorption step (on a time scale of seconds),[19,21−25] most likely due to monolayer formation, followed by a much slower growth (time scales of minutes and hours),[9,24,25] arising from thick multilayer growth. This combination of two processes often leads to either a monolayer with a nonuniform surface coverage or a multilayer of uneven thickness. Optimization of the APS layer, before carrying out step B, was quite difficult.

To overcome this difficulty and to simplify the alignment layer process, we synthesized a new family of silane-based molecules that *contain the photosensitive chromophore as part of the chemical structure*. The molecules are first directly attached to the substrate and then irradiated with linearly polarized light (Path II, Scheme 1). This process leads to the formation of a uniform monolayer useful for liquid crystal alignment.

This paper presents the details of the synthesis of the single-step alignment layer molecules. Detailed results regarding the kinetics of the monolayer formed from these molecules are also presented. Finally, experimental results that demonstrate the alignment of liquid crystals are discussed.

Experimental Section

Materials. Cinnamic acid, aminopropyltriethoxysilane, anhydrous THF, and triethylamine were obtained from Aldrich and used without further purification. The liquid crystals ZLI 4792 were obtained from EM Industries and used as received. The indium tin oxide (ITO) substrates with a coating of 1600 Å of SiO_2 (referred to as passivated ITO) were obtained from Applied Films, Inc. Water was purified with a Nanopure-Ultrapure water system to give a resistivity of 18 MΩ. The deionized water was used for the cleaning procedure, surface chemistry, and static water contact angle measurements.

Techniques. Analytical TLC was conducted on Whatman precoated silica gel 60-F254 plates. ^{1}H NMR spectra (400 MHz) were recorded on a Bruker DRX-400 spectrometer. All spectra were run in $CDCl_3$ or DMSO solutions. The static water contact angle was measured using a goniometer from Rame-Hart, Inc. (model 100-00-115). An automated measurement system using National Instruments Labview (version 3.1) was used for the electrooptic measurements. A white light source or a low-power HeNe laser was used as the source. The transmitted luminance in the normally black or normally white mode was measured using a detector from Graseby Optronics, Inc. (model S370 Optometer).

Surface Modification. An ITO substrate with a coating of 1600-Å SiO_2 and silica wafer substrate were cleaned by first soaking in chloroform and then in a mixture of hydrochloric acid and water (50%/50%) solutions. Each step was performed for 20 min and followed by two rinses with methanol. The substrates were then soaked in concentrated sulfuric acid for 20 min and washed with deionized water. The substrates were then heated in deionized water for 20 min at 80−100 °C.

The cleaned substrates were immersed in a 1% 1 mM solution of acetic acid and combined with 1% of the cinnamate silylating material in anhydrous xylene at room temperature for 1 h. The substrates were then rinsed twice with acetonitrile, finally dried in a nitrogen stream, and stored in a Teflon container.

Irradiation of the Substrates. A 500-W Oriel Mercury arc lamp (power supply 68810, lamp housing 66033, bulb 6285) was used as the UV source. The UV beam was collimated in the setup. A grating monochromator (model 77250) from Oriel

(13) Chu, C. W.; Kirby, P. D. *J. Adhesion Sci. Technol.* **1993**, *7*, 417.
(14) Kang, H.-J.; Blum, F. D. *J. Phys. Chem.* **1991**, *95*, 9391.
(15) Okabayashi, H.; Shimizu, I.; Nishio, E.; O'Connor, C. J. *Colloid Polym. Sci.* **1997**, *275*, 744.
(16) Sudholter, E. J. R.; Huis, R.; Hays, G. R.; Alma, N. C. M. *J. Colloid Interface Sci.* **1985**, *103*, 554.
(17) Trens, P.; Denoyel, R. *Langmuir* **1996**, *12*, 2781.
(18) Tomita, H.; Kudo, K.; Ichimura, K. *Liq. Cryst.* **1996**, *20*, 161.
(19) Vandenberg, E. T.; Bertilsson, L.; Liedberg, B.; Udval, K.; Erlandsson, R.; Elwing, H.; Lundstrom, I. *J. Colloid Interface Sci.* **1991**, *147*, 103.
(20) Kallury, K. M. R.; Macdonald, P. M.; Thompson, M. *Langmuir* **1994**, *10*, 492.
(21) Vrancken, K. C.; Casteleyn, E.; Possemiers, K.; Van Der Voort, P.; Vansant, E. F. *J. Chem. Soc., Faraday Trans.* **1993**, *89*, 2037.
(22) Trens, P.; Denoyel, R.; Rouquerol, J. *Langmuir* **1995**, *11*, 551.
(23) Van Der Voort, P.; Vansant, E. F. *J. Liq. Chrom., Relat. Techol.* **1996** *19*, 2723.
(24) Yoshino, A.; Okabayashi, H.; Shimizu, I.; O'Connor, C. J. *Colloid Polym. Sci.* **1997**, *275*, 672.
(25) Shimizu, I.; Yoshino, A.; Okabayashi, H.; Nishio, E.; O'Connor, C. J. *J. Chem. Soc., Faraday Trans.* **1997**, *93*, 1971.

was used to obtain the irradiation wavelength of 280 nm with a bandwidth of 2.5 nm. A sheet polarizer (model 27320) from Oriel was used to linearly polarize the UV light.

Surface Characterization. Contact angles were measured using a Rame-Hart Model 100-00-115 goniometer The chemical content at the surface was determined by X-ray photoelectro-spectroscopy (XPS). XPS experiments were performed on a Surface Science Instruments SSX-100 surface analysis system with a monochromatic Al Kα source, a hemispherical analyzer, and a position-sensitive detector. Typical pressure in the system during measurement was $\sim 10^{-9}$ Torr. AFM studies were carried out using a Nanoscape IIIa digital instrument. All measurements were performed at room temperature in the tapping mode. We have found that films formed on either silica or ITO surfaces exhibit similar contact angles and surface nitrogen concentrations.

Studies on Liquid Crystals

(a) Cell Preparation. Planar liquid crystal cells were assembled using standard methods. The liquid crystal was ZLI 4792. The thickness of the cell was defined by 20-μm (50 μm for the anchoring energy measurement) thick Mylar spacers. The glass plates used for the cells were patterned with ITO conducting electrodes, 1 cm^2 in area. A thin passivation layer of SiO_2 was deposited on top of the ITO. These surfaces were treated with various photoalignment layers. One of the surfaces did not use a passivation layer. The ITO patterns on the two glass plates that formed the planar cell were made to overlap so that the electric field is uniform over the patterned area. The cells were mounted in the standard antiparallel arrangement. The liquid crystal was injected into the isotropic phase and then slowly cooled into the nematic phase. All measurements were made at room temperature.

(b) Measurement of Contrast. The transmitted intensity of a planar liquid crystal cell placed between crossed polarizers is represented by the following equation,

$$\frac{I}{I_0} = \sin^2(2\chi)\sin^2\left(\frac{\delta}{2}\right)$$

where χ is the angle between the polarizer and the optical axis of the liquid crystal and δ represents the phase shift.

Since the phase shift δ remains constant, the variation in intensity with variation of the angle between the optical axis and polarizer is only due to χ. The contrast is measured by rotating a 20-μm-thick planar cell between crossed polarizers around the axis of the light beam used for measurement. A cell with no contrast would show a flat line while one that shows good contrast shows a good fit to the equation shown. A good fit to the theoretical is hence a quantitative measure of the uniformity of the alignment along a given direction.

(c) Polar Anchoring Strength (*W*). To measure *W*, we have used a modified high-field technique initially suggested by Yokoyama and van Sprang.[26] The modification is in the voltage range used to determine *W*. An electric field is applied to the cell to cause director deviations from the easy direction. Simultaneous measurements of capacitance and optical retardation of the cell allow one to extract the polar anchoring energy. Measurements of the retardation were made using an automated transmission ellipsometer with a resolution of 0.2°. A HeNe laser provided the light source and a Glan Thomson polarizer being used to define the polarization direction of the incident beam. The optic axis of the planar sample was kept at an angle of 45° with respect to the polarizer axis. The phase retardation of the light beam after passing through the sample was measured using a Senarmont ellipsometer. The capacitance was measured as a function of applied voltage at a frequency of 10 kHz. All measurements were performed at room temperature.

Synthesis. Typical procedures of the synthesis of the materials are described below.

(2E)-3-[4-(Alkyloxy)phenyl]-2-propenoic Acid. To a solution of 4-hydroxycinnamic acid (1 mol) in ethanol (95%) was added an excess of sodium hydroxide (2 mol), and the solution was refluxed for 30 min. Bromoalkane (1.1 mol) was then added dropwise, and the mixture was heated overnight at 90 °C. The reaction mixture was then cooled and acidified with 10% HCl aqueous solution. The precipitate was filtered, washed with water, and recrystallized from ethanol. The final product was dried under vacuum to yield **2** as a white solid in 80% yield.

(2E)-3-[4-(Hexyloxy)phenyl]-2-propenoic Acid. mp 149.6−151 °C. ^{1}H NMR ($CDCl_3$) δ ppm: 0.9 (t, 3H, CH_3), 1.32 (m, 4H, $CH_3(CH_2)_2$), 1.45 (m, 2H, $O(CH_2)_2CH_2$), 1.80 (m, 2H, OCH_2CH_2), 4.02 (t, 2H, OCH_2), 6.34 (d, 1H, CH=CHCOO), 6.90 (d, 2H, Ar−H), 7.51 (d, 2H, Ar−H), 7.76 (d, 1H, CH=CHCOO). Elemental analysis, calculated for $C_{15}H_{20}O_3$: C, 72.55; H, 8.12. Found: C, 72.44; H, 8.08.

(2E)-3-[4-(Dodecyloxy)phenyl]-2-propenoic Acid. mp 127.7−128.7 °C. Elemental analysis, calculated for $C_{21}H_{32}O_3$: C, 75.86; H, 9.70. Found: C, 75.84; H, 9.58.

(2E)-3-[4-(Tetradecyloxy)phenyl]-2-propenoic Acid. mp 123.8−125 °C. Elemental analysis, calculated for $C_{23}H_{36}O_3$: C, 76.62; H, 10.06. Found: C, 76.54; H, 10.11.

(2E)-3-[4-(Hexadecyloxy)phenyl]-2-propenoic Acid. mp 122.5−122.9 °C. Elemental analysis, calculated for $C_{25}H_{40}O_3$: C, 77.27; H, 10.38. Found: C, 77.48; H, 10.36.

(2E)-3-[4-(Octadecyloxy)phenyl]-2-propenoic Acid. mp 122.4−122.4 °C. Elemental analysis, calculated for $C_{27}H_{44}O_3$: C, 77.83; H, 10.64. Found: C, 77.97; H, 10.42.

(2E)-3-[4-(Alkyloxy)phenyl]-N-[3-(triethoxysilyl)propyl]-2-propenamide. To a mixture of (1 mol) (2E)-3-[4-(alkyloxy)phenyl]-2-propenoic acid in benzene was added oxalyl chloride (2 mol), a drop of *N*,*N*-dimethylformamide and the solution was stirred overnight at room temperature. The solvent was removed and the crude acid chloride was washed with benzene followed by evaporation of the solvent under a rotovapor. The acid chloride **3** dissolved in anhydrous THF was added dropwise to an ice-cooled solution of 3-aminopropyltriethoxysilane (1 mol) and triethylamine (1 mol) in THF. The reaction mixture was stirred for 1 h under nitrogen, and the precipitate was filtered. The organic filtrate was evaporated under vacuum and the crude product was recrystallized in anhydrous hexane. The product was further purified by flash chromatography on silica gel using ethyl acetate as the eluent, to give **4** in 90% yield.

(2E)-3-[4-(Hexyloxy)phenyl]-N-[3-(triethoxysilyl)propyl]-2-propenamide. mp 66.1−66.8 °C. Elemental analysis,

(26) Yokoyama, H.; Van Sprang, *J. Appl. Phys.* **1985**, *57*, 1985.

Scheme 2

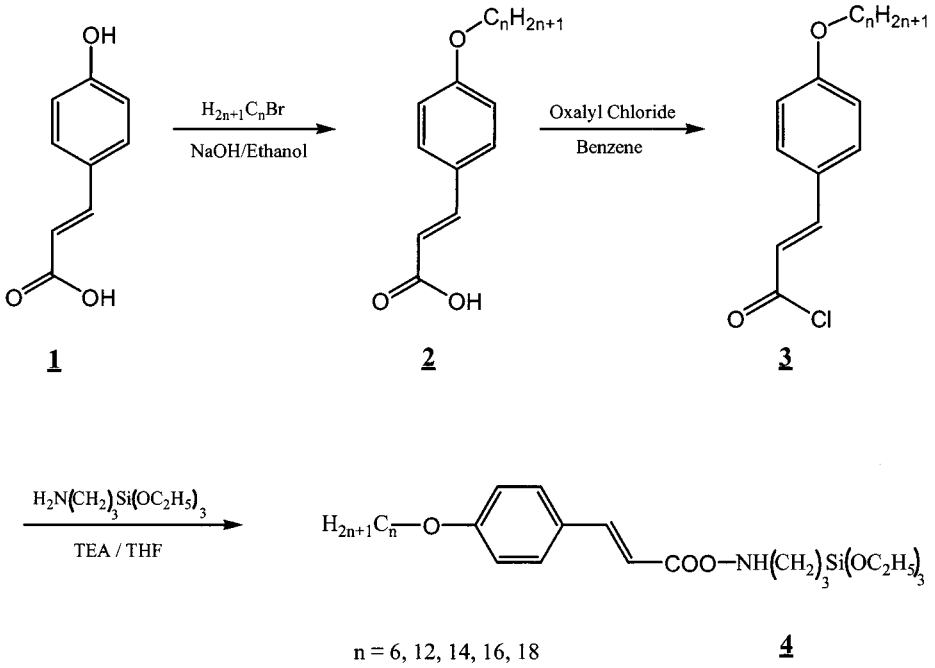

calculated for $C_{24}H_{41}NO_5Si$: C, 63.82; H, 9.15; N, 3.10. Found: C, 63.66, H, 9.03; N, 3.28.

(2E)-3-[4-(Dodecyloxy)phenyl]-N-[3-(triethoxysilyl)propyl]-2-propenamide. mp 53.1−54 °C. Elemental analysis, calculated for $C_{30}H_{53}NO_5Si$: C, 67.25; H, 9.97; N, 2.61. Found: C, 66.99; H, 9.80; N, 2.80.

(2E)-3-[4-(Tetradecyloxy)phenyl]-N-[3-(triethoxysilyl)propyl]-2-propenamide. mp 65.9−66.7 °C. Elemental analysis, calculated for $C_{32}H_{53}NO_5Si$: C, 67.25; H, 9.97; N, 2.61. Found: C, 66.99; H, 9.80; N, 2.80.

(2E)-3-[4-(Hexadecyloxy)phenyl]-N-[3-(triethoxysilyl)propyl]-2-propenamide. mp 82.1−82.9 °C. Elemental analysis, calculated for $C_{34}H_{61}NO_5Si$: C, 68.99; H, 10.39; N, 2.37. Found: C, 69.22; H, 10.24; N, 2.58.

(2E)-3-[4-(Octadecyloxy)phenyl]-N-[3-(triethoxysilyl)propyl]-2-propenamide. mp 76.0−76.7 °C. Elemental analysis, calculated for $C_{37}H_{69}NO_5Si$: C, 69.87; H, 10.39; N, 2.20. Found: C, 69.52; H, 10.62; N, 2.35.

Results and Discussion

Synthesis. The synthesis steps leading to the preparation of the cinnamate monolayers are illustrated in Scheme 2. 4-Hydroxycinnamic acid reacted with bromoalkane in the presence of NaOH to give the monoether derivative **2**. The acid chloride of **2** reacted with APS in THF to yield the final product **4**.

Several homologue materials with different length chains have been prepared. The yield of the last synthetic step has been optimized to 90% or higher. This is in contrast to some low reported yields for similar materials.[18] It was also found that to get high-purity materials, it was necessary to crystallize the compounds in hexane prior to flash chromatography. As shown in Scheme 1, there are two possible pathways leading to the formation of the monolayer. The first pathway (Path 1) relies on the adsorption of APS on the surface followed by reaction of the acid chloride of the chromophore with the amino group of APS. This process actually involves a complex system because the APS molecule is able to interact with the silica surface not only by its amino group but also by the silanol functions resulting from the hydrolysis.[25] Furthermore, it was found via angle-dependent XPS that the amine group is partially protonated and the resulting ammonium group being formed at the silane−glass interface.[27]

The second pathway (Path 2) eliminates in part some of the above-cited problems because it involves reaction of a presynthesized chromophore with the ITO substrates. In this case, APS is already incorporated in the alignment layer, and hence this process reduces the possibility of side reactions.

Contact Angle Studies. All water contact angle studies were made on the SAMs deposited on ITO. In all we have measured the contact angles as a function of the time of deposition for five different silanes (C_6, C_{12}, C_{14}, C_{16}, C_{18}) where C_x represents the number of hydrocarbon atoms attached to the top portion of the alignment layer. It is seen (Figure 1.a) that in all cases the contact angle value attains a saturation value at short deposition times, indicating fast kinetics of the monolayer formation. This is in contrast to the growth curve of APS of the double-step (path I) alignment layer process (Figure 1b). It is also seen that the saturated value of the contact angle exhibits a monotonic dependence in the chain length, the contact angle increasing with increasing hydrocarbon length. This indicates increasing hydrophobicity.

XPS Studies. XPS of film nitrogen was used to determine growth curves for a typical material (C_6) and establish optimum treatment times for subsequent measurements. The N ratio is defined as the surface concentration of N divided by the sum of concentrations of major elements on the surface. Figure 2a shows the absorption growth curve for the C6 material. It is seen that surface nitrogen rises rapidly with short deposition

(27) Pomerantz, M.; Segmuller, A.; Netzer, L.; Sagiv, J. *Thin Solid Films* **1985**, *132*, 153.

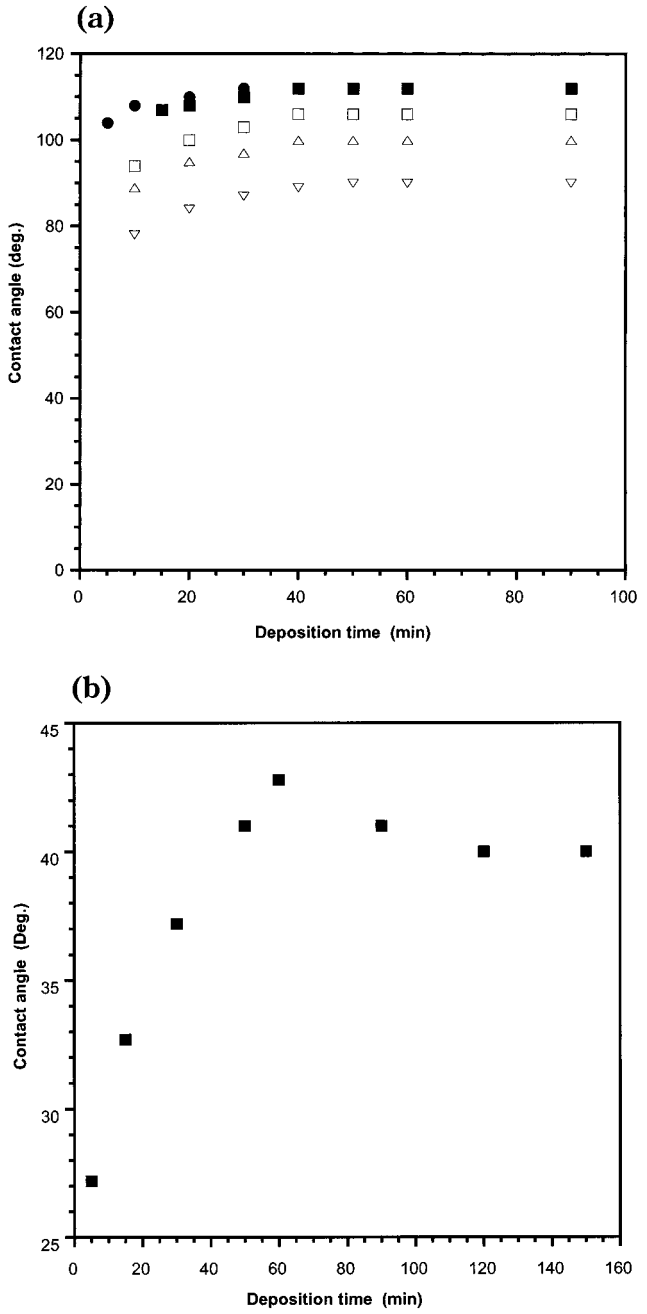

Figure 1. Contact angles of (a) different monolayers(▽, C_6; △, C_{12}; □, C_{14}; ●, C_{16}; ■, C_{18}) and (b) APS, as a function of deposition time.

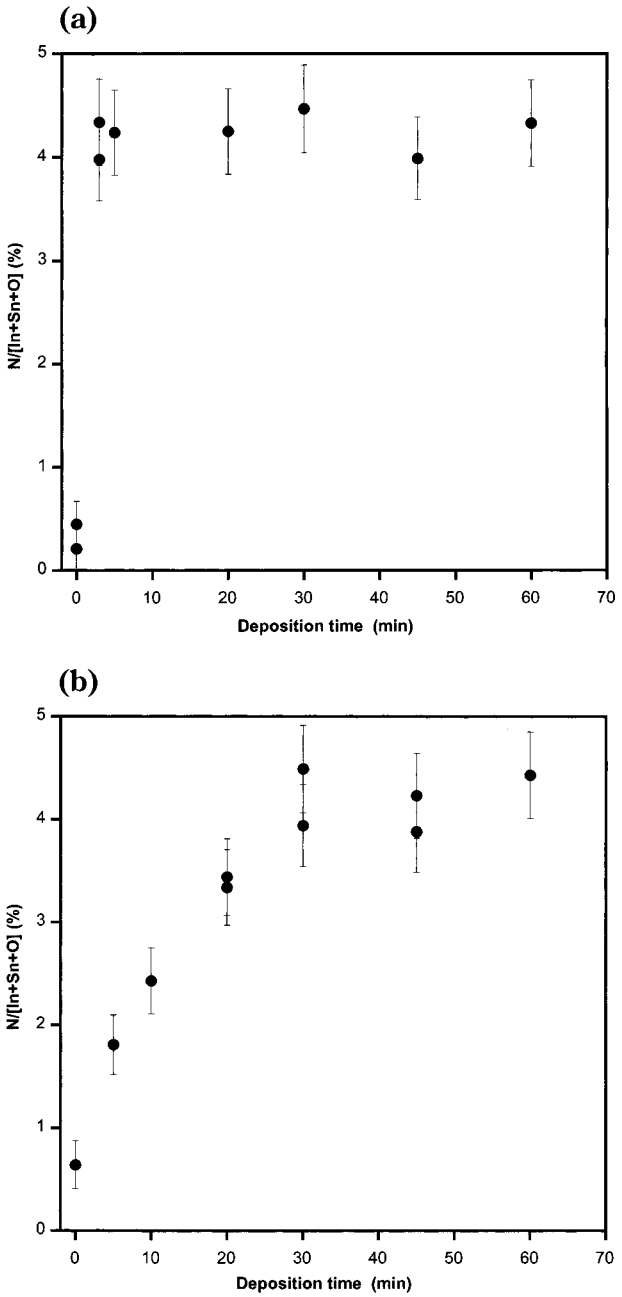

Figure 2. Growth curves of (a) C6 and (b) APS films on ITO. Samples with different treatment times were analyzed by XPS. Multiple measures are from different locations of the same sample. Plotted is surface nitrogen relative to the sum of surface N, In, Sn, and O.

times and saturates at a surface N ratio of ~0.04 within 10 min. In contrast, the XPS data on APS shows a very slow growth curve of the monolayer (Figure 2b), consistent with contact angle results. In our experience the surface concentration value of ≈4.3 seen in Figure 2a is characteristic of well-formed monolayers. Also, there is no indication of further film growth, which would be indicative of multilayer formation. Hence, these results, which are consistent with the contact angle data, show the fast kinetics of the monolayer formation of these new families of silanes.

AFM Studies. We have shown in the previous section that the growth curve for the single-step silane materials (Path II) is extremely fast, the monolayer being formed within minutes. The saturation of the contact angle data as well as the XPS data indicate strongly a well-formed monolayer. We shall now quantify these results by using the AFM technique as a probe of the uniformity of the surface morphology. The AFM studies were conducted using SAMs deposited on silicon wafers. This is to overcome the problems due to the roughness of the ITO surface. We did ascertain that the contact angles for SAMs on ITO and silica wafer are similar so that our deductions based on AFM data for SAMs on the silica wafer are valid for those on the ITO surface as well. Figure 3 shows the AFM images of the C_6 monolayers formed on the silica wafer after different deposition times (30 s, 5 min, 10 min, and 30 min, respectively). Clearly, the surface topography of the monolayer becomes very smooth after a deposition time of 10 min. The root-mean-square (rms) roughness values

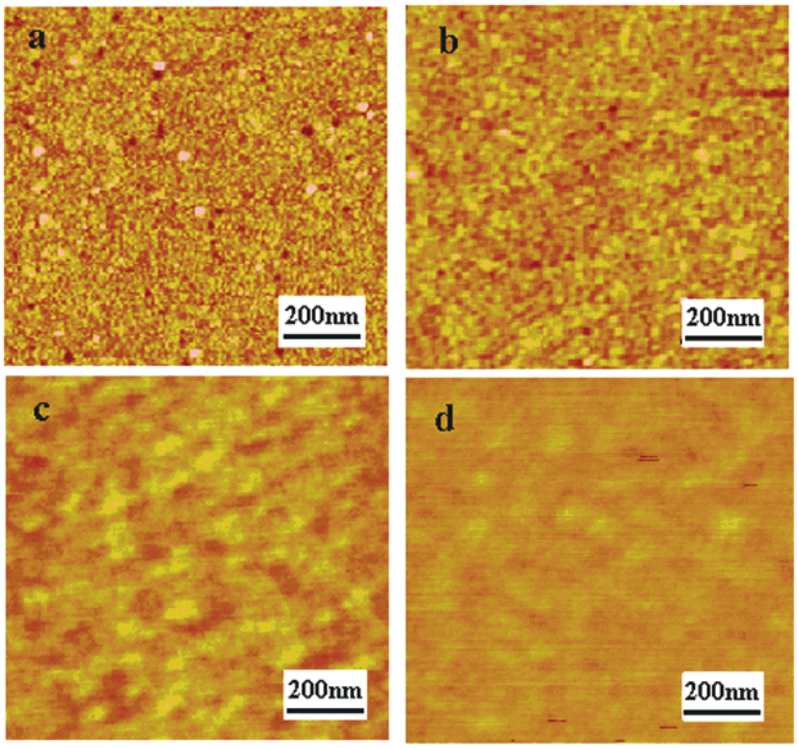

Figure 3. Topographic images of C_6 self-assembled monolayers on a silicon wafer. These monolayers were formed after deposition times of (a) 30 s, (b) 5 min, (c) 10 min, and (d) 30 min.

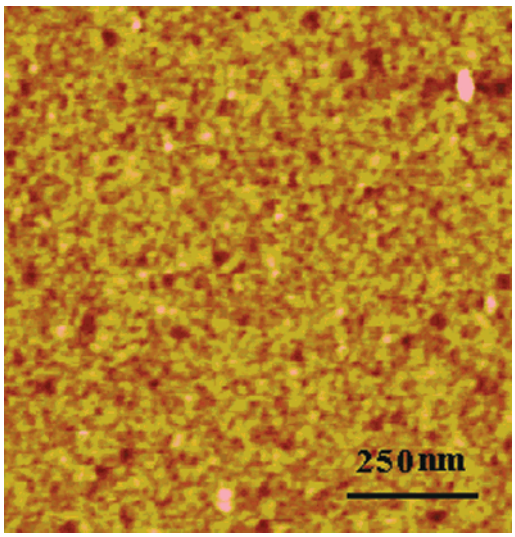

Figure 4. Topographic images of a C_6 monolayer deposed by a two-step process, on a silicon wafer. The monolayer was formed after a 10-min deposition time.

for these monolayers (Figure 3a−d) are 0.23, 0.11, 0.06, and 0.05 nm, respectively. These numbers are the average of seven samples. Hence, within experimental errors (0.02 nm), the roughness reaches an optimal (minimum) value of 0.05 nm after 10 min. This is in striking contrast to the surface topology of a C_6 layer deposited by two-step process (Figure 4). The rms roughness in this case is about 0.2 nm. These results demonstrate that the fast kinetics of the formation of the single-step monolayer alignment material is associated with a well-formed monolayer with a minimal surface roughness.

We have also carried out AFM studies on C_0 and C_{16} (0 and 16 represent the number of hydrocarbon atoms attached at the phenyl ring) monolayers deposited on the silica wafer (Figure 5). The roughness for C_0, C_6, and C_{16} are 0.1, 0.12, and 0.22 nm, respectively. These results suggest that the kinetics of the monolayer formation depends on the chain length of the materials; for example, the growth of the monolayers is fast for short chain silanes. After 30 min, all monolayers reach a minimum rms roughness of 0.05 nm.

Liquid Crystal Alignment and Its Dependence on the Chemical Structure

(a) General Remarks on Alignment. We have studied the nature of liquid crystal alignment for all the alignment layers (C_0, C_6, C_8, C_{12}, C_{14}, C_{16}, C_{18}) using ZLI4792 as the liquid crystal material. To begin with C_0, C_6, and C_8 all give planar alignment. We shall give more details on this in the next section. The quality of alignment (as indicated by the bright state of the planar cell when observed between crossed polarizers, polarizer kept at 45° to the optical axis) appears to be excellent (with a contrast ratio of a least 100:1) for both C_0 and C_6 (Figure 6a), while the alignment is not so good (domains of misaligned regions) for C_8. On the other hand, all the organo-silane materials with longer chain lengths; that is, C_{12}, C_{14}, C_{16}, and C_{18} are found to yield extremely good homeotropic alignment (liquid crystal molecules perpendicular to the alignment substrate) (Figure 6b).

(b) Investigation on Aligned Liquid Crystals. We have conducted two sets of studies to ascertain the quality of the planar alignment and to quantify the strength of the polar anchoring. These factors are relevant to the use of the alignment layers for LC displays. Although we have carried out such studies for C_0, C_4, C_6, and C_8, we shall give here representative data

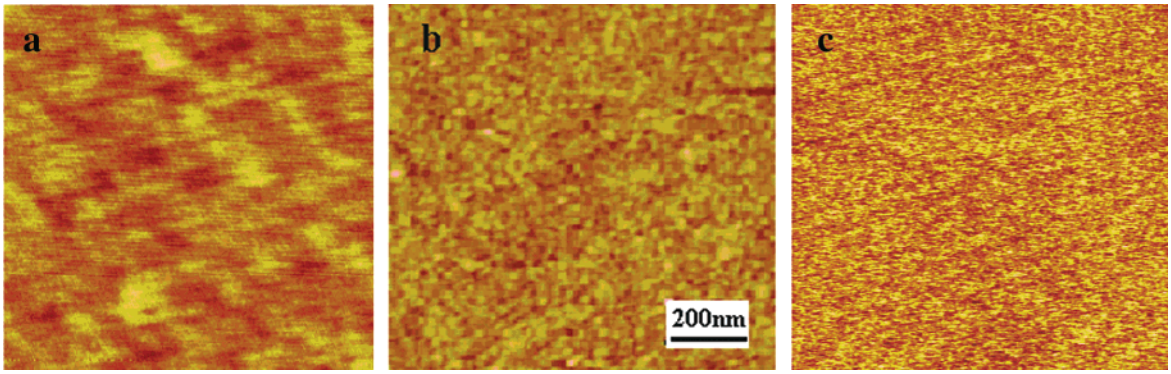

Figure 5. Topographic images of (a) C_0, (b) C_6, and (c) C_{16} self-assembled monolayers on a silicon wafer. All monolayers were formed after a 5-min deposition time. The rms roughness is 0.1, 0.12, and 0.22 nm for C_0, C_6, and C_{16} monolayers, respectively.

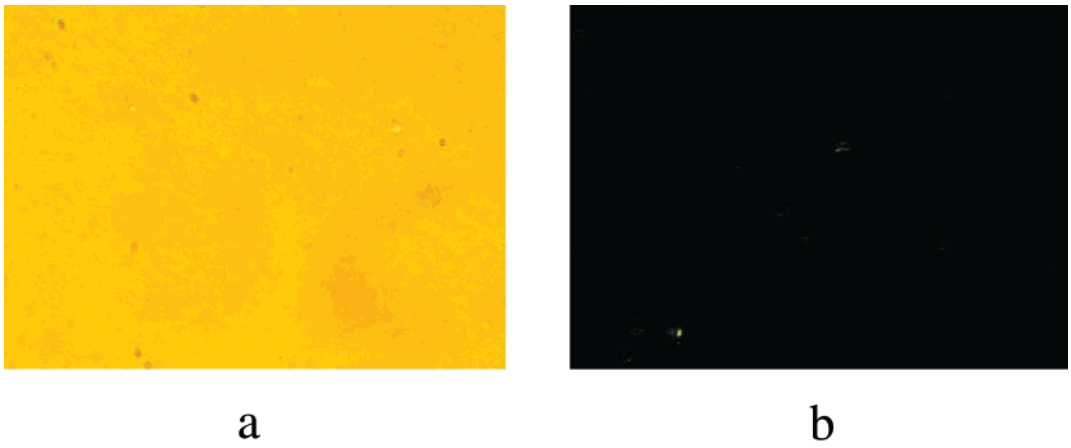

Figure 6. Optical micrographs of a cell filled with ZLI4792 liquid crystal and treated with (a) a C_6 monolayer (planar alignment) observed between crossed polarizers at 45° to the optical axis of the sample and (b) a C_{16} monolayer (homeotropic alignment) viewed along the optical axis of the sample.

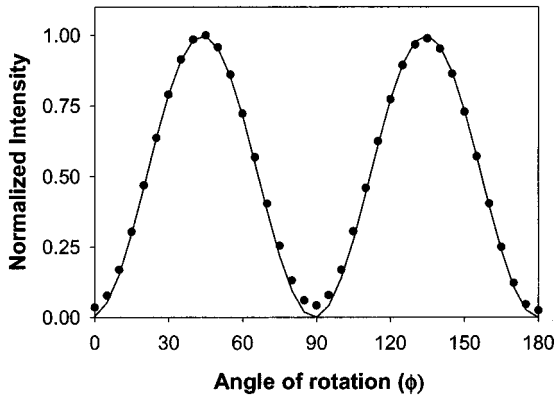

Figure 7. Plot of the normalized intensity as a function of angle of rotation of the cell (ϕ) kept between crossed polarizers. The symbols represent experimental data points and the solid line is a fit to the theoretical equation discussed in the text.

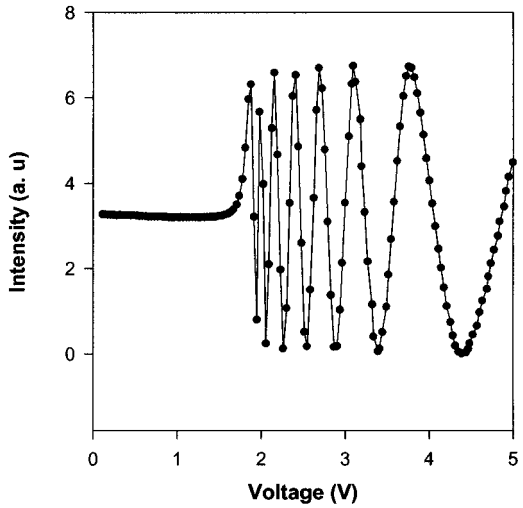

Figure 8. Plot of transmitted intensity as a function of voltage across the 50-μm-thick planar cell. The intensity shows a well defined Freedricksz threshold and then oscillations. These maxima and minima are due to a changing birefringence with voltage and are consistent with the behavior observed in liquid crystal cells that are uniformly aligned.

for one of these (C_6) only. Figure 7 gives a plot of the normalized intensity as a function of angle of rotation of the cell.

The cell is placed such that its optic axis makes an angle of 45° with respect to the polarizer axis, which in turn is crossed with respect to the analyzer. The symbols represent experimental data points and the solid line is a fit to the theoretical equation. Figure 8 gives the plot of transmitted intensity as a function of the voltage across the 50-μm planar cell. The intensity shows a well-defined Freedricksz threshold and then oscillations. These maxima and minima are due to a changing birefringence with voltage and is consistent with the behavior observed in liquid crystal cells aligned uniformly. The data in Figures 7 and 8 clearly establish that the quality of planar alignment is very good.

We shall now present the results of our anchoring energy studies. For our analysis we have used a modified version of the Yokoyama technique[26]. According to

Yokoyama and van Sprang, in a certain range of the cell's parameters and for a certain range of applied voltages, the optical retardation R of the cell changes linearly with the anchoring extrapolation length K_1/W:

$$R = \frac{R_0 I_0(V)}{CV} - \frac{2R_0 K_1}{dW}$$

Here, R_0 is the phase retardation of the cell with no applied field, $I_0(V)$ is a function of voltage and the bulk liquid crystal parameters such as elastic and dielectric constants and refractive indices, C is the capacitance of the cell, V is the applied voltage, K_1 is the splay elastic constant, and d is the thickness of the cell. To extract the polar anchoring strength, the normalized retardation R/R_0 is plotted against $1/CV$ over a certain voltage region and the intercept of the best linear fit to these data determines the extrapolation length and therefore the anchoring strength. More recently, a slightly modified analysis has been used for obtaining the anchoring strength,[28] which requires setting lower and upper limits to the voltage range used. According to this analysis, any deviation of the surface director orientation from the easy axis θ_d requires some work. In the simplest approximation, when the deviations are small and take place in the polar plane, the surface free energy density can be written as

$$F_s = \frac{1}{2} W(\theta - \theta_d)^2$$

where W is the polar anchoring strength and θ is the actual director orientation at the surface. The values of W depend on the nature of both the liquid crystal and the substrate and normally fall in the range from 10^{-2} to 10^{-6} J/m^2.

A plot of the normalized optical phase retardation as a function of the inverse of the product of capacitance times voltage is shown in Figure 9. The data represent a limited voltage range chosen to meet the criterion imposed by the modified Yokoyama method.

The anchoring strength of liquid crystal ZLI 4792 on C6 (A + B) alignment layer is calculated to be 6.6×10^{-5} J/m^2. This is comparable and similar to the planar anchoring strength (6.1×10^{-5} J/m^2) measured using a two-step alignment layer (Path I) reported earlier.

Finally, we shall comment on the switching from planar to homeotropic alignment around C_{10}. It may be recalled that Cognard[29] did an exhaustive study on the aligning influence of different types of silanes on different types of liquid crystals. It appears that in general shorter alkyl chains yield planar alignment while longer chains result in a perpendicular alignment of the liquid crystal molecules. The chemical structure for our alignment layers are however different. Here, we are dealing with "photodimerized monolayers" (PDML) with different chain lengths at the terminal end of the monolayers. Considering that PDML with C_0−C_8 chain length yield a planar alignment while those with C_{12} or longer result in a perpendicular alignment, our results indicate that the primary interactions responsible for the planar LC alignment are probably due to dipolar forces, which are "screened" beyond a certain chain length (C_{10}). For longer chains, the perpendicular alignment is caused by the chain−chain interactions between the LC molecules and the alignment layer. Because the liquid crystal used in our study is ZLI 4792, a multicomponent mixture, it is not possible to make definitive conclusions on the specific nature of the molecular interactions that are responsible for the LC alignment for the C_0−C_8 series. Further studies using single-component polar and nonpolar liquid crystals on similar PDML layers are underway to answer those questions.

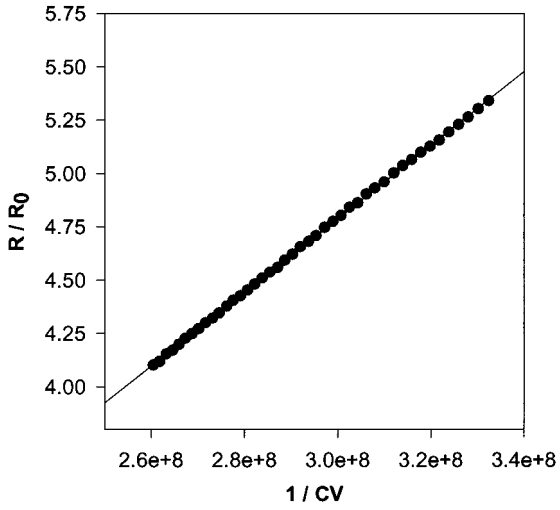

Figure 9. Plot of the normalized optical phase retardation as a function of the inverse of the product of capacitance times voltage. The data represent a limited voltage range chosen to meet the criterion imposed by the modified Yokoyama method.

Acknowledgment. We are very thankful to Dr. Kirsten Grüneburg for her help in some of the experiments. The financial support of the Defense Advanced Research Project Agency and the Office of Naval Research is gratefully acknowledged.

CM000606M

(28) Nastishin, Yu. A.; Polal, R. D.; Shiyanovskii, S. V.; Bodnar, V. H.; Lavrentovich, O. D. *J. Appl. Phys.* **1999**, *86*, 4199.
(29) Cognard, J. *MCLC, suppl. 1* **1982**, 1−77.